

Polarimetry with NICMOS

Dean C. Hines

Steward Observatory, University of Arizona, Tucson, AZ 85721

Abstract. The Near Infrared Camera and Multi-Object Spectrometer (NICMOS) aboard the *Hubble Space Telescope* (HST) incorporates optics in Cameras 1 and 2 (NIC1 and NIC2) that enable high spatial resolution imaging polarimetry at ~ 1 & $2 \mu\text{m}$, respectively. Thermal vacuum tests prior to installation revealed that the three polarizing elements in each camera have unique (non-unity) polarizing efficiencies, and their primary axes are not oriented at the nominal 120° intervals. This non-ideal system requires a reduction algorithm that differs from the standard approach used for ideal polarizers. The coefficients of the algorithm are derived from the ground-based thermal vacuum results and from on-orbit observations of objects of known polarization. The Cycle 7 and 7N calibration resulted in excellent imaging polarimetry performance, capable of producing uncertainties in measured polarization as small as $\sigma_p \approx 1\%$. The Cycle 11 calibration plan includes a recharacterization of the polarimetry capabilities. Herein I review the reduction algorithm, describe the Cycle 11 calibration plan, and present preliminary results. The latter indicate that once fully calibrated, NICMOS will provide polarimetry performance comparable to (or better than) Cycle 7 and 7N. Combined with the polarimetry mode of the Advanced Camera for Surveys (ACS), HST provides high resolution imaging polarimetry from ~ 0.2 – $2.1 \mu\text{m}$. The further possibility of combining imaging polarimetry with coronagraphy in both instruments has the potential to greatly enhance high contrast imaging.

1. Preflight Thermal Vacuum Tests

The NICMOS polarimetry system was characterized on the ground during thermal vacuum tests using a light source that fully illuminated the field of view with completely polarized light and with position angles variable in 5° increments. The primary results of these thermal vacuum tests include:

- Each polarizer in each camera has a unique polarizing efficiency,¹ with POL120S having the lowest at $\epsilon_{\text{POL120S}} = 48\%$.
- Angular offsets between the polarizers within each filter wheel differ from their nominal values of 120° .
- Instrumental polarization caused by reflections off the mirrors in the optical train is small ($\leq 1\%$).
- The grisms act as partial linear polarizers, with G206 producing the largest variation in intensity ($\sim 5\%$) for completely polarized light. Because the grisms reside in the NIC3 filter wheel, they cannot be used with either the NIC1 or NIC2 polarizers and are unsuitable for spectropolarimetry.

¹Polarizer efficiency is defined as $\epsilon = (S_{\text{par}} - S_{\text{perp}})/(S_{\text{par}} + S_{\text{perp}})$, where S_{par} and S_{perp} are the respective measured signals for a polarizer oriented parallel and perpendicular to the position angle of a fully polarized beam.

2. The Algorithm for Reducing NICMOS Polarimetry Observations

The thermal vacuum results showed that the standard reduction algorithm would not work for NICMOS data. Instead, a more general approach was required (Hines, Schmidt & Lytle 1997; Hines, Schmidt & Schneider 2000).

At any pixel in an image, the observed signal from a polarized source of total intensity I and linear Stokes parameters Q and U measured through the k^{th} polarizer oriented at position angle φ_k is

$$S_k = A_k I + \epsilon_k (B_k Q + C_k U) . \quad (1)$$

Here,

$$A_k = \frac{t_k}{2}(1 + l_k), \quad B_k = A_k \cos 2\varphi_k, \quad C_k = A_k \sin 2\varphi_k , \quad (2)$$

ϵ_k is the polarizing efficiency, t_k is the fraction of light transmitted through the polarizer for a 100% polarized input aligned with the polarizer axis, and l_k is the “leak”—the fraction of light transmitted through the polarizer (exclusive of that involved in t_k) when the incident beam is polarized perpendicular to the axis of the polarizer. These quantities are related under the above definitions, $\epsilon_k = (1 - l_k)/(1 + l_k)$.

This treatment can be shown to be equivalent to other approaches, once appropriate transformations are made (Mazzuca, Sparks, & Axon 1998; see also Sparks & Axon 1999).

The values of t_k were determined initially by the filter manufacturer from witness samples, and were not accurately remeasured during thermal vacuum tests. However, on-orbit observations of the unpolarized and polarized standard stars enables refinement of these numbers. Adopted characteristics of the individual polarizers and algorithm coefficients derived during and applicable to Cycle 7 and 7N are listed in Table 1 of Hines, Schmidt & Schneider (2000), and are also available in the NICMOS instrument manual and the *HST Data Handbook*.

After solving the system of equations (eq. 1) for the Stokes parameters at each pixel (I, Q, U), the percentage polarization (p) and position angle (θ) are calculated in the standard way:

$$p = 100\% \times \frac{\sqrt{Q^2 + U^2}}{I}, \quad \theta = \frac{1}{2} \tan^{-1} \left(\frac{U}{Q} \right) . \quad (3)$$

Note that a 360° arctangent function is assumed.

This algorithm has been tested by the NICMOS Instrument Definition Team (IDT) and by the Space Telescope Science Institute (STScI) on several data sets. An implementation has been developed by the IDT, and integrated into a software package written in IDL. The package is available through the STScI web site² and is described by Mazzuca & Hines (1999).

3. The Cycle 11 Polarimetry Characterization Program

The higher, yet more stable, operating temperature provided by the NCS and the three year dormancy of NICMOS may contribute to changes in the properties of the polarimetry optics, especially the t_k coefficients. Therefore, a program to re-characterize the polarimetry optics in Cycle 11 has been developed. The core program has been outsourced by STScI to the author (NIC/CAL 9644: Hines), while flat fields and observations of photometric calibrators are maintained by the NICMOS team at STScI.

The basic design of the program follows the strategy undertaken in Cycle 7 and 7N, relying on observations of polarized and unpolarized standard stars as well as the proto-planetary nebula CRL 2688 (Egg Nebula). The stars are observed at two epochs separated in time such that the spacecraft roll differs by $\sim 135^\circ$. This removes the degeneracy in position angle caused by the

²http://www.stsci.edu/instruments/nicmos/ISREPORTS/isr_99_004.pdf

pseudo-vector nature of polarization. The Egg Nebula is only observed at a single epoch as a direct comparison with observations from Cycle 7 and 7N (ERO 7115: Hines; Sahai et al. 1998; Hines, Schmidt & Schneider 2000), and to evaluate any gross discrepancies across the field of view.

Observations were obtained between UT 2002 September 2 and UT 2002 October 6. The second epoch observations of the polarized and unpolarized standards stars are scheduled between UT 2003 April and UT 2003 July. All observations were obtained using MULTIACCUM sequences and four position spiral dither pattern in each polarizer. The dither pattern used $N+1/2$ ($N \geq 30$) pixel offsets to improve sampling, avoid latent images and mitigate residual instrument artifacts. This is also the recommended observing strategy for all NICMOS polarimetry programs.

4. Preliminary Results of Cycle 11 Polarimetry Characterization Program

The observations were processed through the CALNICA pipeline at STScI using the currently available reference files. The linearity corrections are not yet fully characterized and potentially pose the largest uncertainty in the present results. The flat-fields and the polarimetry calibration images are both potentially affected (this should be corrected soon and will be applied for the final analysis of the complete characterization data set).

Observations of the unpolarized standard star processed with the Cycle 7 and 7N algorithm coefficients yield $p_{\text{NIC1}} = 0.7\% \pm 0.2\%$, $\theta_{\text{NIC1}} = 74^\circ$ and $p_{\text{NIC2}} = 0.7\% \pm 0.3\%$, $\theta_{\text{NIC2}} = 73^\circ$. This suggests that the system may have changed, but the uncertainties are currently too large. The observations of the polarized standard star is also larger ($\Delta p \approx 2\%$) in NIC1 compared with the measurements of Cycle 7 and 7N, which themselves were in excellent agreement with ground-based measurements (Hines, Schmidt & Schneider 2000). The second epoch observations will reduce the uncertainties in the null measurements, and enable the coefficients to be refined.

Observations of the Egg Nebula were also analyzed with the Cycle 7 and 7N coefficients. As for the polarized standard star, the results for the Egg Nebula suggest that the polarimetry system has changed slightly,³ again by about 2% in p%. The Cycle 11 preliminary results are shown in Figure 1. In addition to the traditional polarization vector plot, Figure 1 also shows maps of perpendiculars to the polarization position angle as a function of position in the Egg Nebula. Perpendicular maps show the direction of the illuminating source relative to the last scattering surface as projected on the sky. The convergent points in the Cycle 11 data are consistent with the Cycle 7 and 7N data (Weintraub et al. 2000), and indicate no significant field-dependent anomalies in the polarimetry system.

5. Summary

The Cycle 11 re-characterization plan is partially complete. The preliminary results indicate that the coefficients of the algorithm for deriving Stokes parameters from images taken through the NICMOS polarizers will require slight adjustment after all of the standard star observations have been completed in the Spring of 2003. Observations of the Egg Nebula suggest that, once fully calibrated, NICMOS will provide polarimetry performance comparable to (or better than) Cycle 7 and 7N. Combined with the polarimetry mode of the Advanced Camera for Surveys (ACS), *HST* provides high resolution imaging polarimetry from ~ 0.2 – $2.1 \mu\text{m}$. The further possibility of combining imaging polarimetry with coronagraphy in both instruments has the potential to greatly enhance high contrast imaging.

³The polarization structure of the Egg is not expected to change over the 5 year period between observations even though the object is known to show photometric variations.

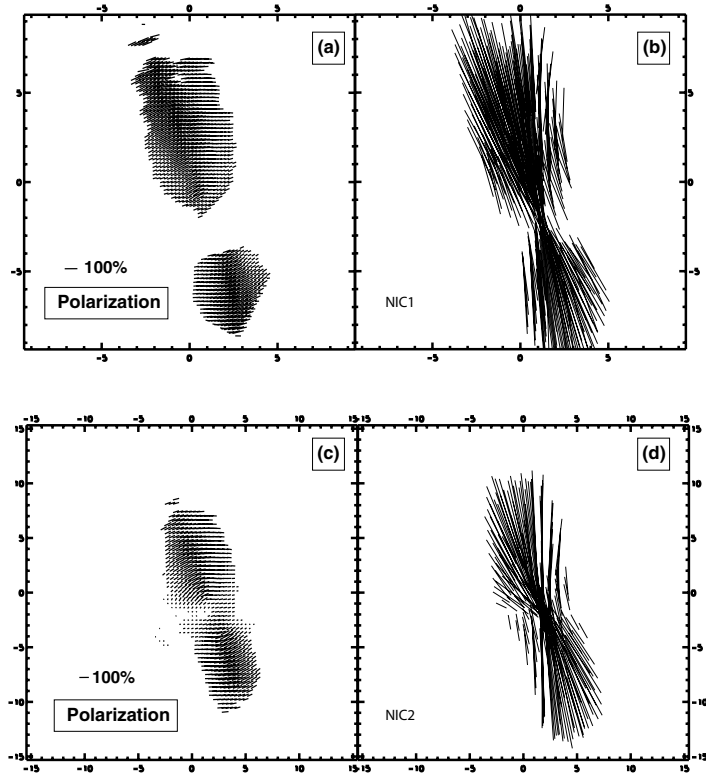


Figure 1. Cycle 11 polarimetry observations of the Egg Nebula (CRL 2688). The left-side panels show the polarization maps, while the right-side panels show the perpendiculars to the polarization position angles (see text).

References

- Hines, D. C., Schmidt, G. D., & Lytle, D. 1997, in *The 1997 HST Calibration Workshop*, eds. S. Casertano et al. (Baltimore: STScI)
- Hines, D. C., Schmidt, G. D., & Schneider, G. 2000, *PASP*, 112, 983
- Mazzuca, L., Sparks, B., & Axon, D. 1998, *Instrument Science Report NICMOS-98-017* (Baltimore: STScI)
- Mazzuca, L. & Hines, D. C. 1999, *Instrument Science Report NICMOS-99-004* (Baltimore: STScI)
- Sahai, R., Hines, D. C., Kastner, J. H., Weintraub, D. A., Trauger, J. T., Rieke, M. J., Thompson, R. I., & Schneider, G. 1998, *ApJ*, 492, L163
- Sparks, W. B. & Axon, D. J. 1999, *PASP*, 111, 1298
- Weintraub, D. A., Kastner, J. H., Hines, D. C., & Sahai, R. 2000, *ApJ*, 531, 401